

Electronic Supplementary Information

Ultrahigh power output and durable flexible all-polymer triboelectric nanogenerators enabled by rational surface engineering

Ying-Ying Chen, T. S. T. Balamurugan, Chih-Yu Chang*, Chih-Yuan Hsu, Chih-Yu Fang, Yi-Shan Liu, Li-Fu Ho

Department of Materials Science and Engineering, National Taiwan University of Science and Technology, Taipei, 10607, Taiwan (R.O.C.) (E-mail: cychang@gapps.ntust.edu.tw)

Table S1. Comparison of the output characteristics of state-of-the-art semi-transparent TENG as well as the present work.

Source	Triboelectric materials	V_{oc} [Volt]	I_{sc} [μ A]	Power density [$W\ m^{-2}$]
Reference 1	IL + PDMS	150	45	3
Reference 2	SF coated PET + PET	213.9	—	0.068
Reference 3	Electric wire + PVC gel	24.7	0.83	0.087
Reference 4	Graphene + nest-like porous PDMS	271	7.8	0.975
Reference 5	Chitosan and starch mixture + FEP	1080	27	5.07
Reference 6	AgNW + PDMS	66	8.6	0.446
Reference 7	PUA + AgNW-embedded PEDOT:PSS	160	≈50	15
Reference 8	Al + FP	444.8	44.2	0.818
This work	PEDOT:PSS/cPLL + PDMS/F ₁₇ polymer	688	33.0	13.4

Abbreviation: IL, ionic liquid; SF-coated PET, silk-fibroin patch-film on the polyethylene terephthalate; PVC, polyvinyl chloride; FEP, fluorinated ethylene propylene; AgNW, silver nanowires; PUA, polyurethane acrylate; FP, fluoropolymer.

Note: “—” in the table implies that the data are not recorded in research.

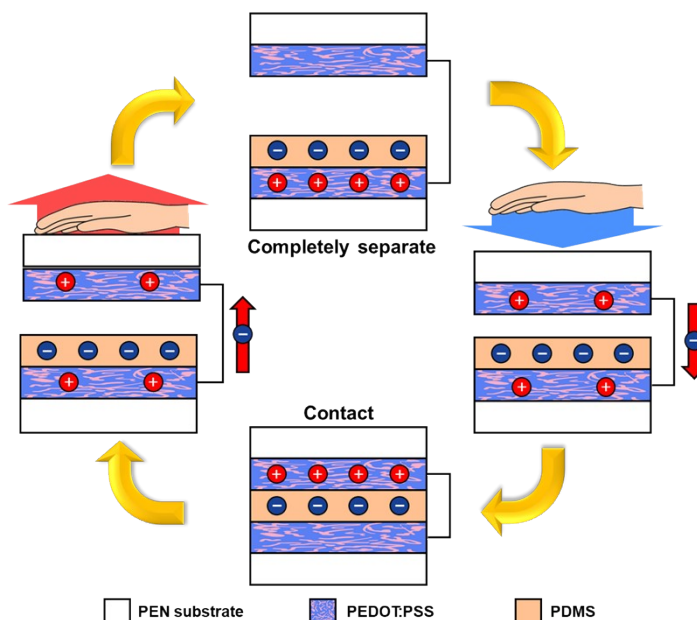


Fig. S1. Schematic illustration of the working principle of TENG investigated in this study.

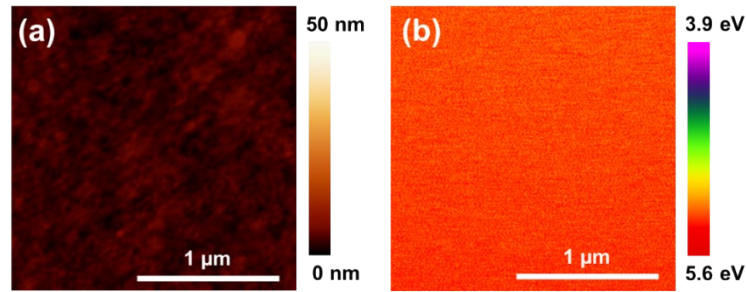


Fig. S2. (a) AFM topographic and (b) KPFM images of PEDOT:PSS layer.

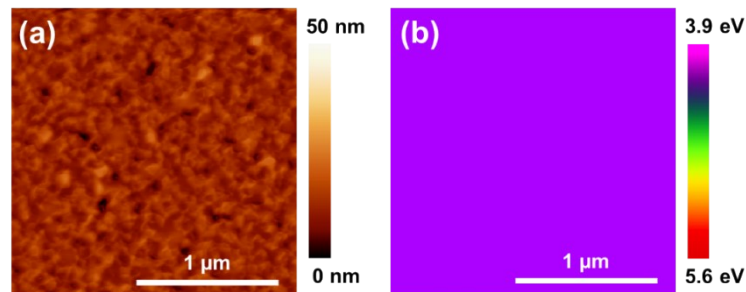


Fig. S3. (a) AFM topographic and (b) KPFM images of Al layer.

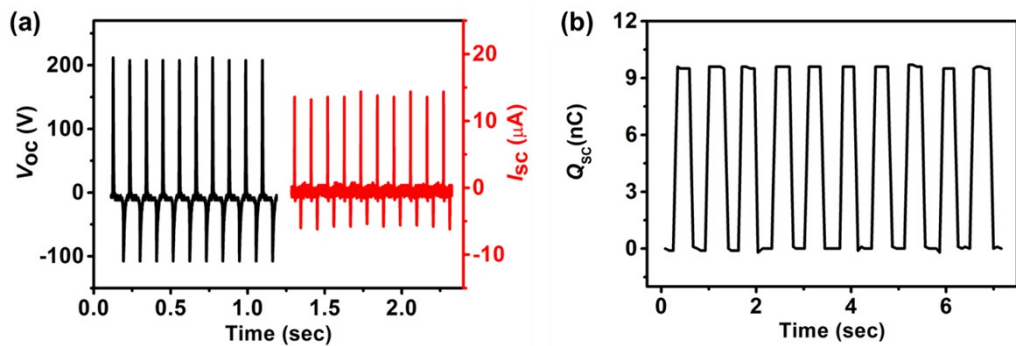


Fig. S4. Output characteristics of as-fabricated TENG with PDMS dielectric layer and Al electrode: (a) V_{oc} and I_{sc} , and (b) Q_{sc} .

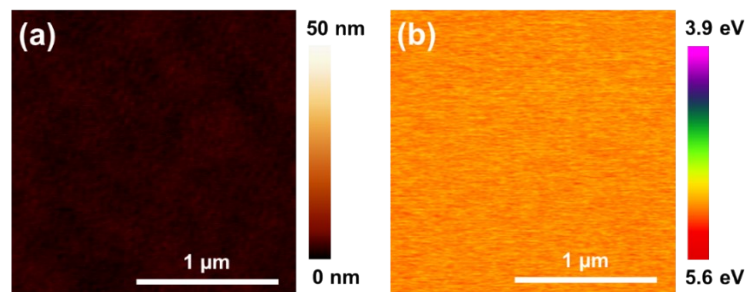


Fig. S5. (a) AFM topographic and (b) KPFM images of PDMS layer.

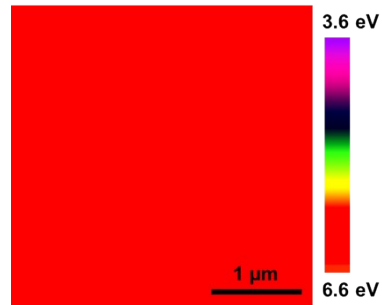


Fig. S6. KPFM image of PDMS/F₁₇ SAM sample.

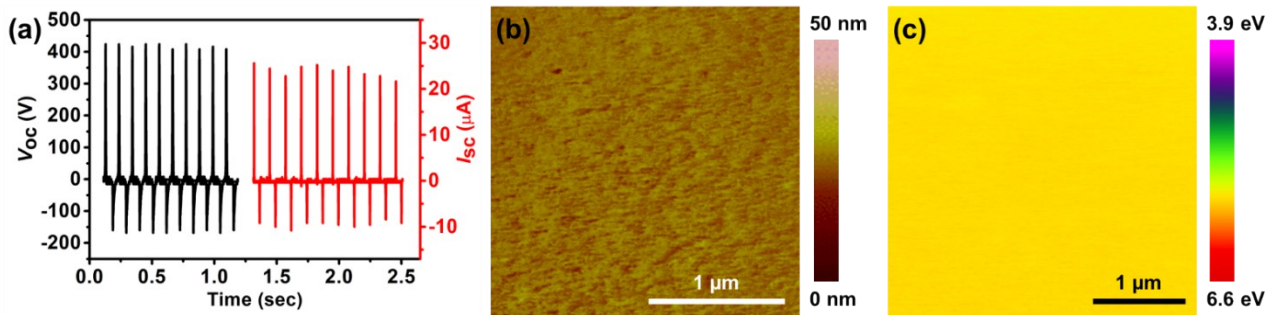


Fig. S7. (a) Output characteristics of as-fabricated all-polymer flexible TENG based on F₁₇ polymer processed under ambient air. (b) AFM topographic and (c) KPFM images of PDMS layer.

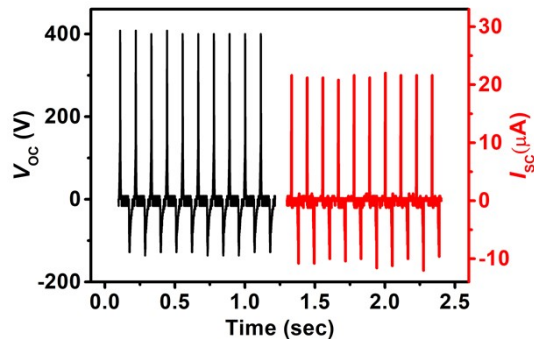


Fig. S8. Output characteristics of as-fabricated F₁₇ polymer-functionalized PDMS TENG using Al electrode ($V_{oc} = 408$ V, $I_{sc} = 21.6$ μ A)

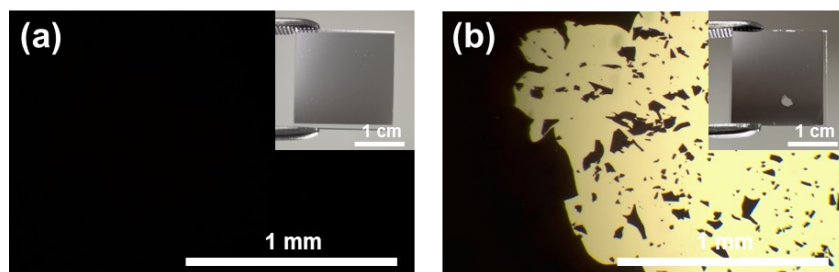


Fig. S9. Optical microscope images and digital images (inset) of Al electrode layer: (a) before, and (b) after 200,000 cycles of continuous operation.

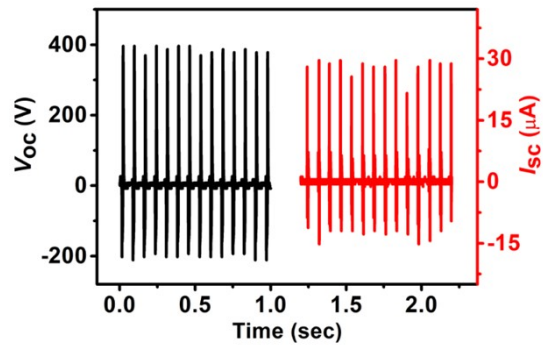


Fig. S10. Output characteristics of as-fabricated TENG based on F_{17} SAM modification layer.

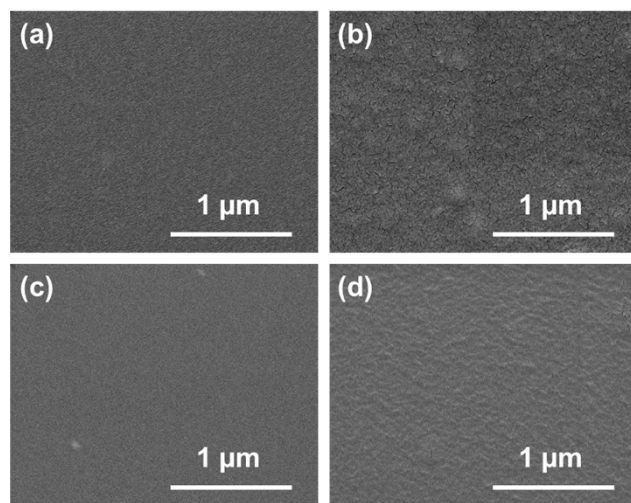


Fig. S11. SEM images of the samples before (left panel) and after (right panel) 200,000 cycles of continuous operation: (a, b) PDMS/ F_{17} polymer and (c, d) PEDOT:PSS/cPLL.

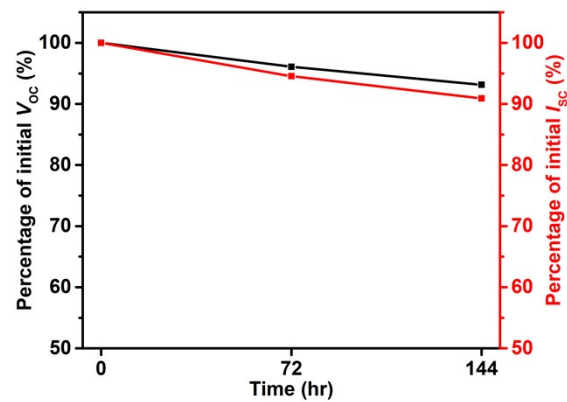


Fig. S12. Evolution of V_{oc} and I_{sc} of as-fabricated all-polymer flexible TENG (Device D) as a function of storage time under humid ambient conditions (25 °C, relative humidity = 70-80%).

References

1. Y. Kim, D. Lee, J. Seong, B. Bak, U. H. Choi and J. Kim, *Nano Energy*, 2021, **84**, 105925.
2. C. Liu, J. Li, L. Che, S. Chen, Z. Wang and X. Zhou, *Nano Energy*, 2017, **41**, 359-366.
3. H. Park, S.-J. Oh, D. Kim, M. Kim, C. Lee, H. Joo, I. Woo, J. W. Bae and J.-H. Lee, *Advanced Science*, 2022, **9**, 2201070.
4. X. He, X. Mu, Q. Wen, Z. Wen, J. Yang, C. Hu and H. Shi, *Nano Res.*, 2016, **9**, 3714-3724.
5. Z. Zheng, D. Yu, B. Wang and Y. Guo, *Chem. Eng. J.*, 2022, **446**, 137393.
6. X. Liang, T. Zhao, W. Jiang, X. Yu, Y. Hu, P. Zhu, H. Zheng, R. Sun and C.-P. Wong, *Nano Energy*, 2019, **59**, 508-516.
7. B.-Y. Lee, S.-U. Kim, S. Kang and S.-D. Lee, *Nano Energy*, 2018, **53**, 152-159.
8. B. Kim, J. Y. Song, D. Y. Kim, M.-c. Kim, Z.-H. Lin, D. Choi and S. M. Park, *Nano Energy*, 2022, **104**, 107878.